OPTIMAL CONFIGURATIONS FOR ROTATING SPACECRAFT FORMATIONS

Steven P. Hughes* **and Christopher D. Hall†**

In this paper we introduce a new class of formations that maintain a constant shape as viewed from the Earth. We develop an algorithm to place n spacecraft in a constant shape formation spaced equally in time using the classical orbital elements. To first order the dimensions of the formation are shown to be simple functions of orbit eccentricity and inclination. The performance of the formation is investigated over a Keplerian orbit using a performance measure based on a weighted average of the angular separations between spacecraft in formation. Analytic approximations are developed that yield optimum configurations for different values of n. The analytic approximations are shown to be in excellent agreement with the exact solutions.

INTRODUCTION

Clusters of low-performance spacecraft flying in formation may provide enhanced performance over single high-performance spacecraft. This is especially true for remote sensing missions where interferometry or stereographic imaging may provide higher resolution data. There are many possibilities for configuring formations of satellites for such missions, but there are relatively few established performance measures for evaluating the effectiveness of particular configurations. This is especially important as configurations vary during an orbit due to orbital dynamics, and over longer time scales due to perturbations.

Significant attention has been given in the literature to many aspects of the distributed spacecraft concept. A preliminary feasibility study of formation flying technologies was performed by Folta *et al.* [1]. At the time of study it was determined that limitations in pointing accuracy could not meet an 80% overlap in the presence of errors. Further investigations were performed by Folta *et al.* [2] to understand how to relate observations from two spacecraft, to determine the effects of perturbations, and to confirm previous results. The formation flying concept was revisited by Folta *et al.* [3] in 1996 and the feasibility of formation flying for particular missions in light

*Graduate Research Assistant; Currently, Aerospace Engineer, Guidance, Navigation, and and Control Center, NASA Goddard Space Flight Center, (301) 286-0145, (301) 286-0369 (FAX), email: shughes@pop500.gsfc.nasa.gov

†Assistant Professor, Department of Aerospace and Ocean Engineering, Virginia Tech., (540) 231-2314, (540) 231-9632 (FAX), email: chall@aoe.vt.edu

of new advances in technology and autonomy was investigated. The dynamics of an uncontrolled formation with and without atmospheric drag was studied.A formation control strategy for the Earth Observing System-AM1 (EOS-AM1) and Landsat-7 was investigated using a dynamic ballistic coefficient strategy.

DeCou [4] developed a three-satellite station-keeping strategy describing paths to perform very long baseline optical interferometry. DeCou concluded that the thrusting required is low enough to allow missions of up to ten years using ion thrusters without refueling. Gramling *et al.* [5] demonstrated the possibility of using Goddard Space Flight Center's (GSFC) Onboard Navigation System (ONS) for relative navigation of the EO-1/Landsat-7 spacecraft formation. Hartman *et al.* [6] extended the study of GSFC's ONS performance for spacecraft formation flying. Specifically Hartman investigated orbit determination and prediction accuracies and their impact on the relative separation errors.

The use of GPS for relative navigation of formation flying spacecraft has been studied by Guinn *et al.* [7] and for both relative position and attitude sensing by Adams *et al.* [8] and How *et al.* [9]. Adams *et al.* [8] presented results from a GPS-based relative navigation and attitude sensing system developed in the laboratory.

In this paper we introduce a class of formations we call rotating formations, where the configuration remains relatively constant during an orbit. We present a detailed analysis of the performance of this class of formations, including an approximate analytical determination of the optimal configuration based on an angular performance measure. The new class of formations involves an elliptical arrangement of satellites in slightly elliptical orbits, each inclined slightly with respect to the orbital plane of the reference circular orbit. Each orbit has the same semimajor axis, inclination with respect to the reference plane, eccentricity, and argument of periapsis. The position of each satellite is determined by these common elements, and by unique values for the right ascension of the ascending node and true anomaly at epoch. We develop general expressions for these angles in terms of the number of satellites in the formation, n, based on a equal-time distribution of the satellites. The relative configuration remains nearly constant during an orbit, as the satellites rotate about the reference circular orbit. In our development, the eccentricity e and inclination i are treated as design variables, and we are interested in choosing values that optimize an appropriate performance measure.

One measure of the performance of such a formation is the angular separation between the satellites, as this defines the performance of interferometry and of stereographic imaging. A particular instrument's effectiveness in these missions can be related to the angular separation, α_{ij}, between the i_{th} and j_{th} satellites in the formation. For a specific value, α_m, the performance of any pair of satellites will be maximized. Since the angular separation varies during the orbit, the performance measure is actually an orbit-averaged quantity depending on all the angular separations. For

the rotating configuration developed here, the integrand of this performance measure is nearly constant, especially for large n, since the time it takes the formation to reach a nearly equivalent configuration is T/n, where T is the orbital period. Thus we can use the integrand as a proxy performance measure, which allows the analytical development of the measure with all orbital elements included in the expression.

The full analytical expression of the performance measure is extremely complicated, and its complexity increases geometrically with n. We develop a relationship between the eccentricity and inclination that permits us to develop a series approximation for the performance measure. Using only terms to second order, we develop simple approximations for the values of e and i that maximize the formation performance. These approximations take the form of a function that depends only on n multiplied by the optimal separation angle α_m. Thus the optimal e and i can easily be computed for the different optimal separation angles associated with different instruments. The approximations exhibit excellent agreement with the exact solutions obtained using the orbit-averaged "exact" version of the performance measure. Furthermore, the functional dependence of the optimal e and i on the number of satellites, n, is recaptured by investigating the solutions for different values of n.

DEVELOPMENT OF THE ROTATING FORMATION

In this section we develop a formation of n spacecraft so that the satellites move along an ellipse-like shape in a relative reference frame. A configuration of n spacecraft on an ellipse-like path is shown in Figure 1. In general we define the horizontal dimension as the longitudinal separation and the vertical separation as the latitudinal separation. The dimensions can be physically represented using the angular or spatial separations. To distinguish between the two representations we measure the size of the ellipse using the angle δ_{lon} to specify the longitudinal angular separation and δ_{lat} to specify the latitudinal separation. We use a similar convention to express the dimensions of the ellipse in units of distance. When we discuss the dimensions of the motion in units of distance the horizontal dimension is termed d_{lon} and the vertical dimension is called d_{lat}. We show that to first order the dimensions of the formation are simple functions of orbit eccentricity and inclination.

In our development of the rotating formation we use two coordinate systems: an inertial frame $\mathcal{F}_R$, and a relative reference frame $\mathcal{F}_{rel}$ defined by a reference circular orbit. We choose the reference circular orbit to be equatorial with a true longitude at epoch of ℓ_{ref}. The origin of $\mathcal{F}_{rel}$ is attached to a reference spacecraft that moves along the reference orbit. The x_{rel}-axis is in the direction of the reference spacecraft's position vector. The y_{rel}-axis lies along the reference spacecraft's velocity vector direction. By this definition the y_{rel}-axis is always tangent to the reference orbit. The z_{rel}-axis is chosen to complete the right-handed set, and is in the orbit normal direction.

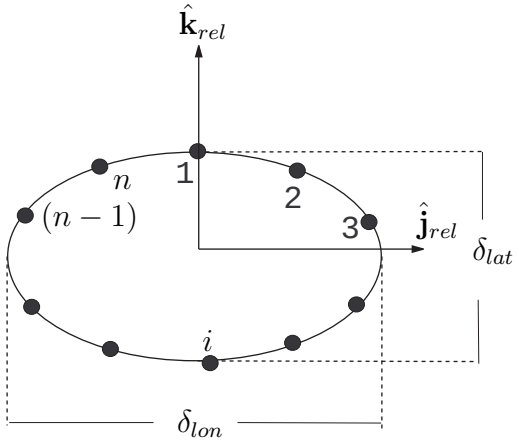

Figure 1: Geometry of the Rotating Formation

Frame $\mathcal{F}_R$ is an inertial frame but it is not equivalent to the Earth-centered inertial frame $\mathcal{F}_I$ commonly found in the literature. The frame is fixed in inertial space with its origin at the center of the Earth. However, its axes can be defined by any arbitrary right-handed system. The result is that the x_R-y_R plane of $\mathcal{F}_R$ is not the Earth's equatorial plane, it is the orbital plane of the reference circular orbit. The orbital elements used to describe the rotating formation are used according to their classical definition, but for generality they are measured with respect to $\mathcal{F}_R$ unless otherwise stated.

We wish to determine the dimensions of the relative orbit in terms of the orbital elements of the spacecraft in formation. To simplify the analysis we limit our discussion to orbits that are nearly circular and result in small displacements from the reference orbit. In doing so we require that the spacecraft motion occurs in nearly the same plane as the reference motion. Therefore, the along-track displacements in the relative motion are primarily due to the eccentricity of the orbits. With these assumptions we can determine the dependence of δ_{lon} and δ_{lat} on the orbital elements.

We see in Figure 2 a view of the ellipse-like path of the rotating formation shown in $\mathcal{F}_R$. The vector $\mathbf{r}_1$ describes the position of an arbitrary spacecraft. The true anomaly, ν, for the spacecraft is measured from the $\hat{\mathbf{i}}_1$ axis. The quantity y_{lon} is the along-track component of angular separation of the spacecraft in $\mathcal{F}_{rel}$; i.e., y_{lon} is defined as an angle and not a distance. From inspection of Figure 2 we see that the angle δ_{lat} is due to the difference in inclination between the orbit and the reference orbit. The expression for δ_{lat} in terms of the inclination is simply

$$\delta_{lat} = 2i \tag{1}$$

Recall that we assume the out-of-plane motion does not affect the along-track angular separation. Therefore we can determine δ_{lon} by investigating the projection

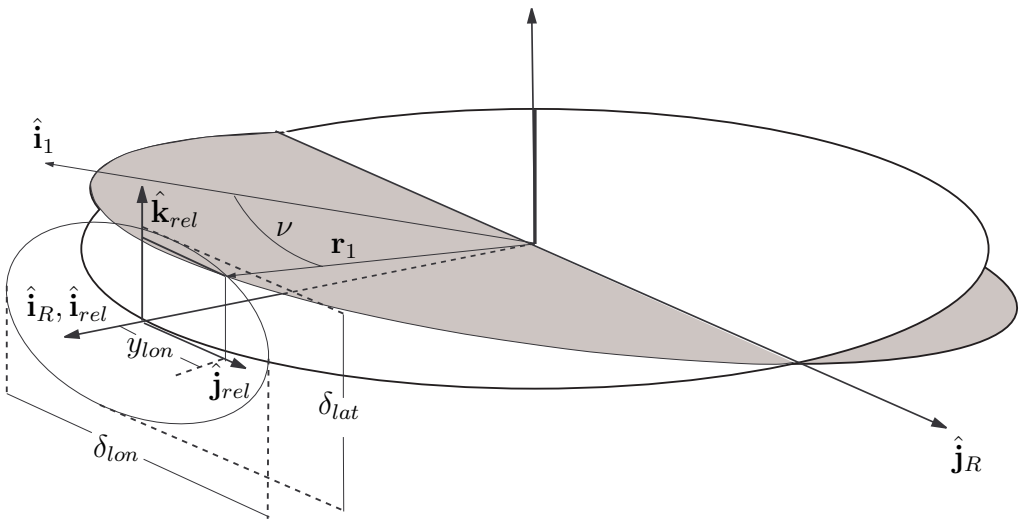

Figure 2: The Rotating Formation Seen in $\mathcal{F}_R$ and $\mathcal{F}_{rel}$

of the motion in the $x_R - y_R$ plane as seen in Figure 3. To determine δ_{lon} we must first develop an expression for y_{lon}. From inspection of Figure 3 we can write

$$y_{lon} = \nu - \theta \tag{2}$$

where θ is the angle between $\hat{\mathbf{i}}_{rel}$ and $\hat{\mathbf{i}}_1$. We can express θ as

$$\theta = M_{0_{rel}} + \eta t \tag{3}$$

where $M_{0_{rel}}$ is the angle between $\hat{\mathbf{i}}_{rel}$ and $\hat{\mathbf{i}}_1$ at the initial epoch. The horizontal dimension, δ_{lon}, is simply twice the maximum in the along-track separation:

$$\delta_{lon} = 2y_{lon}|_{max} \tag{4}$$

For small e we can write

$$\nu = M_{0_1} + \eta t + 2e \sin\left(M_{0_1} + \eta t\right) \tag{5}$$

as found in Vallado [10], where M_{0_1} is the mean anomaly of $\mathbf{r}_1$ at the initial epoch, and η is the mean motion. Substituting Eqs. (3) and (5) into Eq. (2) we obtain

$$y_{lon} = 2e \sin\left(M_{0_1} + \eta t\right) + M_{0_1} - M_{0_{rel}} \tag{6}$$

Recall that M_{0_1} and $M_{0_{rel}}$ are constants so

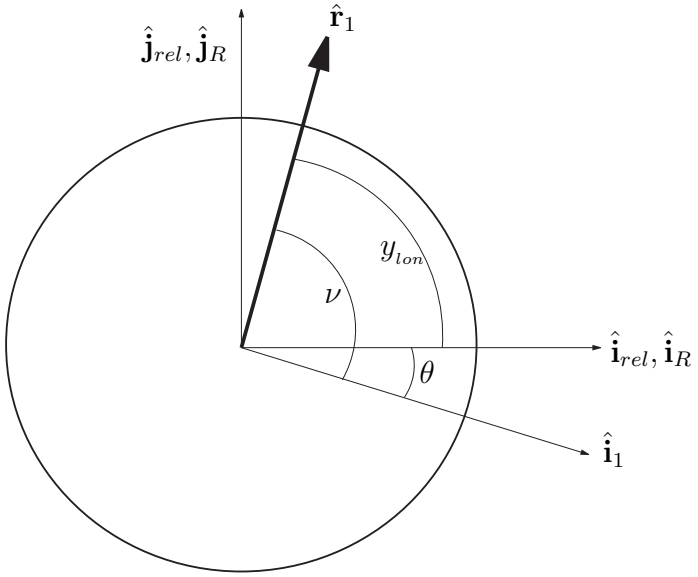

Figure 3: The Rotating Formation Projected into the $x_R - y_R$ Plane

$$y_{lon}|_{max} = 2e \tag{7}$$

Substituting Eq. (7) into Eq. (4)we obtain

$$\delta_{lon} = 4e \tag{8}$$

A similar result was arrived at by Chichka [11] using a second-order approximation.

We now know the dimensions of the rotating formation in terms of e and i. However, we need to develop an algorithm to place n spacecraft in an ellipse-like formation defined by δ_{lon} and δ_{lat}.

SPACECRAFT PLACEMENT IN THE ROTATING FORMATION

Knowing δ_{lon} and δ_{lat} we wish to develop an algorithm to place n spacecraft along the ellipse-like path in the relative reference frame. The spacecraft can be placed in the formation in three different configurations: equal angle separations, equal arc length separations, and equal time separations. We develop an algorithm to place the spacecraft around the ellipse-like path with equal time separations. For circular formations, equal time separation is equivalent to equal arc length and equal angle separation. For ellipse-like formations the relationship between the three configurations is non-trivial. We develop the formation by first investigating the requirements to place a single spacecraft on an ellipse-like path defined by δ_{lon} and δ_{lat}. Then we generalize the method to include n spacecraft spaced equally in time.

We know from Eqs. (1) and (8) that the dimensions of the relative motion path in $\mathcal{F}_{rel}$ depends only on e and i. Therefore, for all the spacecraft to move along an

ellipse of the same dimensions in $\mathcal{F}_{rel}$, all the orbits in the formation must have a common e and i. Solving for i in Eq. (1) yields

$$i = \delta_{lat}/2 \tag{9}$$

From Eq. (8) the eccentricity can be written as

$$e = \delta_{lon}/4 \tag{10}$$

To ensure a cohesive formation, all the orbits must also have the same semimajor axis. Therefore, only the argument of periapsis, ω, the longitude of ascending node, Ω, and the true anomaly, ν may vary for the orbits in the rotating formation.

In Figure 4 we see the position of an arbitrary satellite at two different epochs. At the initial epoch the position is described by $\mathbf{r}_{t_0}$; at a later epoch the position is described by $\mathbf{r}_{t_i}$. We choose the origin of the reference orbital frame to lie along the x_R-axis at the initial epoch in a circular orbit whose plane of motion is the $x_R - y_R$ plane. We begin constructing the formation by placing a spacecraft in position 1 shown in Figure 1. The relative motion is chosen to be clockwise. For clockwise motion to occur the spacecraft at position 1 must be moving in the y_{rel} direction faster than the origin of the reference orbit. Therefore, we place spacecraft 1 at the periapsis of its orbit:

$$\nu_1 = 0 \tag{11}$$

We must choose ω_1 and Ω_1 to position the periapsis of orbit 1 over $\hat{\mathbf{i}}_R$. By inspection of Figure 4 we see that this is accomplished by choosing

$$\Omega_1 = 3\pi/2 \qquad \omega_1 = \pi/2 \tag{12}$$

In summary, the orbital elements to position a spacecraft at position 1 in $\mathcal{F}_{rel}$ at the initial epoch are

$$a_1 = a \quad e_1 = \delta_{lon}/4 \quad i_1 = \delta_{lat}/2 \quad \omega_1 = \pi/2 \quad \Omega_1 = 3\pi/2 \quad \nu_1 = 0 \tag{13}$$

We now wish to generalize the algorithm to place n satellites spaced equally in time along the ellipse-like path seen in Figure 1. For all satellites to move along the same path in $\mathcal{F}_R$ we require that all the orbits share a common a, e, and i. However, we must determine ω, Ω, and ν for the remaining orbits.

The time of separation, t_s, between spacecraft in an equal time formation is given by

$$t_s = T/n = \frac{2\pi}{n}\sqrt{\frac{a^3}{\mu}} \tag{14}$$

To determine the orbital elements of the i^{th} spacecraft in formation we propagate orbit 1 through time t_i where

$$t_i = (i-1)t_s \tag{15}$$

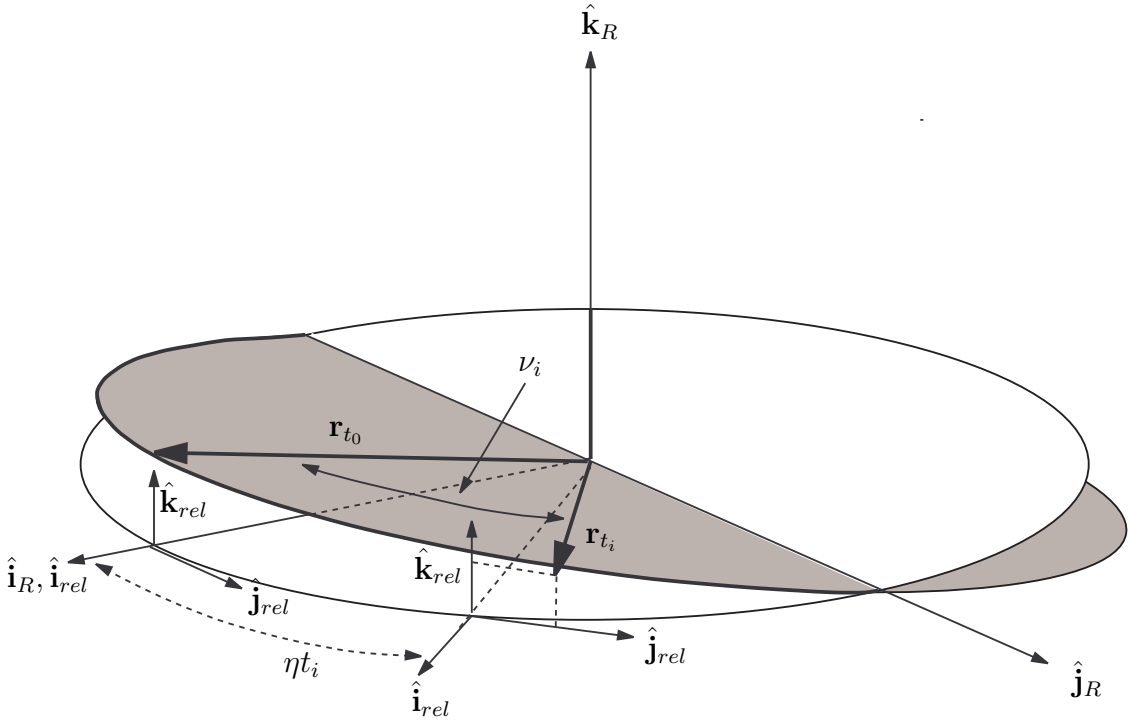

Figure 4: Time Evolution of the Rotating Formation

The configuration of spacecraft 1 and the reference orbit at the initial epoch, t_0, and at t_i can be seen in Figure 4. We need to determine ν_{t_i}, the value of ν for orbit 1 after the passage of time t_i. For small e we can write

$$\nu_{t_i} = M_{t_i} + 2e \sin M_{t_i} \tag{16}$$

where

$$M_{t_i} = M_0 + (i-1)\eta t_s \tag{17}$$

Recall that the true anomaly for orbit 1 at the initial epoch is zero. Therefore, we know that $M_0 = 0$. Substituting Eq. (14) and (17) into Eq. (16) we obtain

$$\nu_{t_i} = \frac{2\pi}{n}(i-1) + 2e \sin\left(\frac{2\pi}{n}(i-1)\right) \tag{18}$$

For a Keplerian orbit only ν changes with time. Therefore we now know the orbital elements to space n spacecraft equally in time in $\mathcal{F}_R$. However, we are interested in the elements that yield n spacecraft spaced equally in time in $\mathcal{F}_{rel}$. Therefore, we need to determine the new configuration of $\mathcal{F}_{rel}$ after the passage of time t_i. Then we can determine the orbital elements to space n spacecraft equally in time in $\mathcal{F}_{rel}$ by a coordinate transformation.

The frame $\mathcal{F}_{rel}$ is defined by a circular, equatorial reference orbit in $\mathcal{F}_R$. Therefore the motion of the coordinate system $\mathcal{F}_{rel}$ after time t_i is simply a 3-rotation through

the angle $\theta = \eta t_i$. Performing a 3-rotation through ηt_i to $\mathcal{F}_{rel}$ is equivalent to rotating Ω_i through an angle $\theta = -\eta t_i$. Therefore to have n spacecraft spaced equally in time in $\mathcal{F}_{rel}$ we write

$$\Omega_i = 3\pi/2 - \eta t_i = \frac{3\pi}{2} - \frac{2\pi(i-1)}{n} \tag{19}$$

In summary, to obtain the orbital elements to place the i^{th} spacecraft in an equal time, rotating formation in $\mathcal{F}_{rel}$ we propagate orbit 1 through t_i as defined in Eq. (15). Then we rotate the longitude of the ascending node backwards through ηt_i to Ω_i as defined by Eq. (19) to account for the motion of $\mathcal{F}_{rel}$. Hence a, e, i, and ω are the same for all orbits in the formation. The true anomaly and the longitude of ascending node are given by Eqs. (18) and (19). In general, the i^{th} set of orbital elements is given by

$$\begin{gathered} a_i = a \quad e_i = \delta_{lon}/4 \quad i_i = \delta_{lat}/2 \quad \omega_i = \pi/2 \quad \Omega_i = 3\pi/2 - \tfrac{2\pi(i-1)}{n} \\ \nu_i = \tfrac{2\pi}{n}(i-1) + 2e_i \sin\left(\tfrac{2\pi}{n}(i-1)\right) \end{gathered} \tag{20}$$

where $1 \leq i \leq n$.

PERFORMANCE OF THE ROTATING FORMATION

We wish to investigate the performance of the rotating formation using an appropriate metric. We propose that the performance of the formation can be evaluated by investigating the angular separations between spacecraft over the course of an orbit[12]. Specifically, an orbit-averaged quantity based on the sum of the instantaneous separation angles is considered:

$$W_\alpha = \frac{1}{n_s T} \int_0^T \sum_{i=1}^{n-1} \sum_{j=i+1}^{n} w_\alpha(\alpha_{ij})\, dt \tag{21}$$

where w_α is an instantaneous position metric to be chosen by the analyst, α_{ij} is the angular separation between the i^{th} and j^{th} spacecraft, and η_s is the number of unique separation angles given by

$$n_s = \frac{n^2 - n}{2} \tag{22}$$

A measure of this form allows the analyst to define an instantaneous metric for the angular separation between a pair of spacecraft. The performance of all pairs in formation is evaluated accordingly and summed together to obtain a measure of the formation performance at a particular instance in time. By integrating the instantaneous metric over an orbit we obtain a measure of orbit effectiveness. We choose a parabolic form for the instantaneous weight function, w_α. In doing so we can choose an upper and lower limit for the acceptable angular separations between two spacecraft as well as the optimum configuration for two spacecraft.

To solve the performance problem we need the position information for all spacecraft in formation over an orbit period. In general spacecraft are subject to forces from the spherical primary as well as perturbations from atmospheric drag, solar radiation pressure, third body forces, and non-spherical effects. However, for a preliminary analysis we approximate the orbital dynamics with Keplerian motion. Therefore to obtain the conditions that yield an optimum configuration we must solve for an optimum in Eq. (21) where the dynamics of the formation are described by the two body equation of motion with the initial conditions given by the orbital elements in Eq. (20).

We now investigate optimum configurations of the formation according to the angular separation performance metric.

An Analytic Solution

We wish to determine optimal configurations of the rotating formation in terms of the orbital elements defining the rotating formation. Hence, we seek the orbital elements that yield an optimum in Eq. (21). In general W_α does not permit a closed-form analytic solution. However we may make some simplifying assumptions and apply the metric to the rotating formation to obtain analytic results. We wish to find a closed-form solution for the maximum in Eq. (21) where

$$w_\alpha(\alpha_{ij}) = c_1\alpha_{ij}^2 + c_2\alpha_{ij} + c_3 \tag{23}$$

The performance measure seen in Eq. (21) is based on the angular separations between spacecraft, which are determined by the orbital elements in Eq. (20). For the rotating formation the orbital elements are simple functions of a, n, δ_{lon}, and δ_{lat}. However, the angular separation between spacecraft does not change with semimajor axis. Therefore we can write

$$\alpha_{ij} = f(n, \delta_{lon}, \delta_{lat}) \tag{24}$$

The parabolic instantaneous weight function, w_α, can be uniquely defined by three constants c_1, c_2, and c_3. The result is that the performance problem has six design variables such that

$$W_\alpha = f(n, \delta_{lon}, \delta_{lat}, c_1, c_2, c_3) \tag{25}$$

We can solve for δ_{lon} and δ_{lat} in terms of inclination and eccentricity therefore we can express α_{ij} in terms of n, e, and i. A solution for α_{ij} in terms of n, e, and i allows a solution for W_α of the form

$$W_\alpha = f(n, e, i, c_1, c_2, c_3) \tag{26}$$

We use the cross product to obtain an expression for α_{ij}:

$$\| \mathbf{r}_i \times \mathbf{r}_j \| = r_i r_j \sin \alpha_{ij} \tag{27}$$

For close formations α_{ij} is small so we can assume

$$\sin \alpha_{ij} \approx \alpha_{ij} \tag{28}$$

Solving for α_{ij} we obtain the expression

$$\alpha_{ij} = \frac{\| \mathbf{r}_i \times \mathbf{r}_j \|}{r_i r_j} \tag{29}$$

We can write the vector $\mathbf{r}_i$ in the perifocal system as

$$\mathbf{r}_{i_p} = \frac{a(1-e^2)}{1 + e\cos\nu_i} \begin{bmatrix} \cos\nu_i & \sin\nu_i & 0 \end{bmatrix}^T \tag{30}$$

where ν_i and ν_j are given by Eq. (20). The vector $\mathbf{r}_j$ can be expressed using a similar expression by replacing the subscript i in Eq.(30) with j.

To use Eq. (29) we must rotate the vectors into a common reference frame using the appropriate rotation matrix. We can construct the rotation matrix to go from the perifocal system to $\mathcal{F}_R$ for the i^{th} position vector using

$$\mathbf{R}_i^{Ip} = \mathbf{R}_3(-\Omega_i)\mathbf{R}_1(-i)\mathbf{R}_3(-\omega) \tag{31}$$

where Ω_i is given in the orbital element set in Eq. (20). Then we can write the inertial representations of $\mathbf{r}_i$ and $\mathbf{r}_j$ using

$$\mathbf{r}_{i_I} = \mathbf{R}_i^{Ip}\mathbf{r}_{i_p} \qquad\qquad \mathbf{r}_{j_I} = \mathbf{R}_j^{Ip}\mathbf{r}_{j_p} \tag{32}$$

Using the preceding, we have the information required to evaluate α_{ij} from Eq. (29). The expression, which is not shown here, is a non-trivial transcendental function of the form

$$\alpha_{ij} = f(n, e, i) \tag{33}$$

We now make some assumptions to arrive at a simpler form for W_α.

Simplifying Assumptions

In general, solving W_α requires integrating the motion over an orbit. However, for special configurations of the rotating formation, the relative spacing between the

spacecraft is nearly constant over an orbit. This is true for near circular rotating formations when

$$\delta_{lon} \approx \delta_{lat} \tag{34}$$

The relative positions are also nearly constant over an orbit for formations composed of a large number of spacecraft. In Figure 5 we see a rotating formation of four spacecraft. The shaded circles represent the positions of four spacecraft at the initial epoch. The white circles represent the positions of the spacecraft after a small passage of time, Δt . The relative positions, and hence the angular separations, have changed after the time Δt. However, when the spacecraft at position 1 reaches posi-

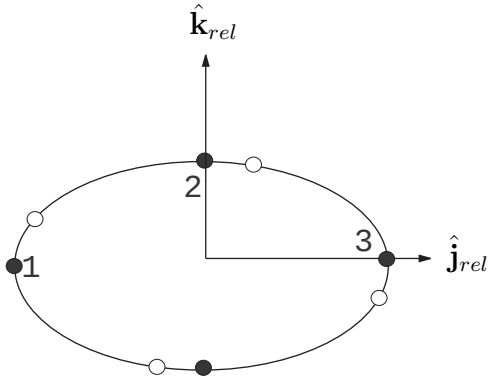

Figure 5: Rotating Formation of Four Spacecraft

tion 2 the relative positions of the spacecraft will be nearly the same as at the initial epoch. The relative positions are not exactly the same because all of the spacecraft in formation are at different points in elliptical orbits. For example, for this configuration spacecraft 2 is at periapsis and spacecraft 1 is at a true anomaly given by Eq. (20) with $i = 4$. Therefore the time for spacecraft 1 to reach position 2 is slightly different from the amount of time for spacecraft 2 to reach position 3. For a four-spacecraft formation the relative positions are nearly the same after a passage of time $T/4$. In general, for a formation of n spacecraft, the relative positions are nearly equivalent after time T/n. Therefore the period of the formation decreases with n. More importantly though, as n increases the amplitude of the integrand in Eq. (21) goes to zero. This is demonstrated in Figure 6. We see a plot of the integrand over an orbit period for $n = 4, 6, 10$. The plot was created for a highly elliptical formation with $d_{lon} = 6000$ m and $d_{lat} = 1000$ m. As n increases we see that the period and amplitude of the motion decrease. Hence, the relative positions of the spacecraft are nearly constant for large n.

If the relative motion of a formation is nearly constant over an orbit we can neglect the integral in

$$W_\alpha = \frac{1}{\eta_s T} \int_0^T \sum_{i=1}^{n-1} \sum_{j=i+1}^{n} w(\alpha_{ij})\, dt \tag{35}$$

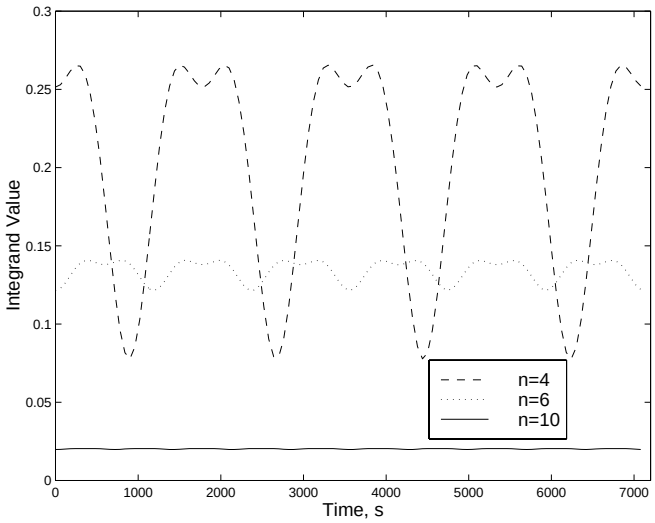

Figure 6: Integrand *vs.* Time for a Highly Elliptical Formation

and express W_α as $\tilde{W}_\alpha$ where

$$\tilde{W}_\alpha = \frac{1}{\eta_s} \sum_{i=1}^{n-1} \sum_{j=n+1}^{n} w(\alpha_{ij}) \tag{36}$$

With Eqs. (23), (29), and (36) we have the tools to express W_α analytically. We are interested in the dimensions of the rotating formation that result in optimum performance. Recall that the shape of the rotating formation is determined by e and i. The analytic expression of W_α is a non-trivial function in terms of six variables. We wish to simplify the expression to solve for optimum configurations in terms of e and i. Recall that W_α is not dependent on a. Therefore we can continue the analysis without concern for the specific value of semimajor axis.

To obtain an expression for W_α we need to evaluate the summation in Eq. (36) for a given n. We choose $n = 4$ to demonstrate the techniques used to obtain the optimum. We then present results for several values of n to determine trends in the optimum solutions for changing n.

Assuming $n = 4$ in Eqs. (23), (29), and (36), we can express W_α in terms of e, i, c_1, c_2, and c_3. We can expand the expression to third-order in small e and i about $e = 0$ and $i = 0$ to obtain an approximate expression. However, the resulting expression has a singularity at $e = 0$. Plotting the exact expression for W_α in negative i and e, as shown in Figure 7, lends some understanding: there is a cusp at $e = 0$ and $i = 0$. We need to expand about another point where there is no singularity. To do so we make a substitution using

$$e = \frac{i}{2}(1 + \epsilon) \tag{37}$$

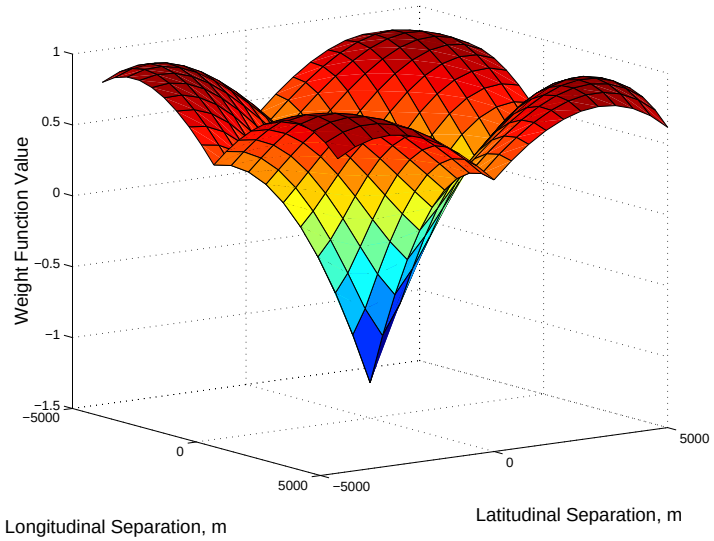

Figure 7: The Singularity in Eccentricity

where $0 < \epsilon \ll 1$ is a small dimensionless parameter. This substitution eliminates the singularity in e. Expanding the resulting expression to third-order in i and ϵ yields an approximate expression for W_α:

$$W_a = -\left(\frac{11c_2}{18} + \frac{13c_2}{18\sqrt{2}}\right) i^3 + \frac{8c_1 i^2 \epsilon}{3} + \frac{8c_1 i^2}{3} + \frac{c_2 \epsilon^2 i}{6\sqrt{2}} + \left(\frac{\sqrt{2}c_2 + c_2}{3}\right) \epsilon i + \frac{2\sqrt{2}c_3 + 2c_2}{3} + c_3 \tag{38}$$

To solve for the e and i resulting in an optimum we must solve the set of simultaneous equations

$$\frac{\partial W_a}{\partial i} = 0 \qquad\qquad \frac{\partial W_a}{\partial e} = 0 \tag{39}$$

for e and i. However, we first must find expressions for $\partial W_a/\partial i$ and $\partial W_a/\partial e$ in terms of e. Differentiating Eq. (38) with respect to i yields

$$\frac{\partial W_a}{\partial i} = \frac{64c_1(1+\epsilon)i + c_2(8(1+\sqrt{2}) + 4(1+\sqrt{2})\epsilon + \sqrt{2}\epsilon^2 - (22+13\sqrt{2})i^2}{12} \tag{40}$$

To obtain an expression in terms of e we substitute using

$$\epsilon = 2\frac{e}{i} - 1 \tag{41}$$

to obtain

$$\frac{\partial W_a}{\partial i} = \frac{128c_1 e i^2 + c_2(4\sqrt{2}e^2 + 4(2+\sqrt{2})ei + i^2(4 + 5\sqrt{2} - (22+13\sqrt{2})i^2))}{12i^2} \tag{42}$$

Taking the partial derivative of W_a with respect to ϵ yields

$$\frac{\partial W_a}{\partial \epsilon} = \frac{i^2\left(c_2(2 + 2\sqrt{2} + \sqrt{2}\epsilon) + 16c_1 i\right)}{12} \tag{43}$$

To determine an expression in terms of e we multiply by $\partial\epsilon/\partial e$ where

$$\frac{\partial \epsilon}{\partial e} = 2/i \tag{44}$$

The derivative with respect to e is

$$\frac{\partial W_a}{\partial e} = \frac{\partial W_a}{\partial \epsilon}\frac{\partial \epsilon}{\partial e} = \frac{i\left(16c_1 i^2 + c_2\left(2\sqrt{2}e + (2+\sqrt{2})i\right)\right)}{12} \tag{45}$$

Solving Eqs. (42) and (45) simultaneously for e and i we obtain expressions for e and i that yield an optimum in W_α. The expressions are complex and not shown here. However, there is a relation between the optimum e and i such that

$$e_{opt} = i_{opt}/2 \tag{46}$$

Recall that we assume $n = 4$ in order to obtain an explicit expression for W_α. Therefore Eq. (46) appears to be dependent on the assumption that we have a four spacecraft formation. However, if we assume $n = 2, 3, 4, 5, 6, 8, 10$ we obtain the same result.

We now investigate the physical implications of Eq. (46). Substituting the relations for e and i from Eq. (20) into Eq. (46) we see that $\delta_{lon} = \delta_{lat}$. Hence the ideal rotating formation according to W_α is circular.

For a circular formation we can make an additional simplification by writing

$$e = i/2 \tag{47}$$

Substituting Eq. (47) into Eq. (36) yields an expression for W_α in terms of n, i, c_1, c_2, and c_3. Recall that the only assumptions made to arrive at Eq. (36) are small angles and that the integrand in Eq. (35) is constant in time. To simplify W_α we expand in a power series to second-order in i. We investigate a larger formation with $n = 8$. A second order expansion in i for $n = 8$ yields

$$W_a = \frac{16c_1}{7}i^2 + c_2\left(\frac{4}{7\sqrt{2-\sqrt{2}}} + \frac{2\sqrt{2}}{7} + \frac{2}{7}\right)i + c_3 \tag{48}$$

To provide a more intuitive understanding of the results we introduce a new form for the parabolic weight function seen in Eq. (23):

$$w_\alpha(\alpha_{ij}) = \frac{1}{\alpha_s}(\alpha_{ij} - \alpha_u)(\alpha_{ij} - \alpha_l) \tag{49}$$

where α_u and α_l are the upper and lower limits on angular separation respectively and α_s is a normalization factor. The constants c_1, c_2, and c_3 from Eq. (23) can be

written in terms of α_u, α_l, and α_s using

$$c_1 = 1/\alpha_s \tag{50}$$
$$c_2 = -(\alpha_u + \alpha_l)/\alpha_s \tag{51}$$
$$c_3 = \alpha_u \alpha_l / \alpha_s \tag{52}$$

For circular formations the radius of the formation is simply the inclination of the orbits composing the formation. Therefore, solving for the optimum radius, r_o, from Eq. (48) and substituting for c_1, c_2, and c_3 using Eqs. (50–52) we obtain

$$r_o = \left(\frac{1}{16} + \frac{\sqrt{2}}{16} + \frac{1}{16} \left(\sqrt{2 - \sqrt{2}} + \sqrt{2 + \sqrt{2}} \right) \right) (\alpha_l + \alpha_u) \tag{53}$$

We define a new angle, α_m, such that

$$\alpha_m = \frac{\alpha_u + \alpha_l}{2} \tag{54}$$

This angle is the ideal separation angle according to the instantaneous weight function w_α. We can rewrite r_o in terms of α_m:

$$r_o = \left(\frac{1}{8} + \frac{\sqrt{2}}{8} + \frac{1}{8} \left(\sqrt{2 - \sqrt{2}} + \sqrt{2 + \sqrt{2}} \right) \right) \alpha_m \tag{55}$$

We apply the same techniques to find the optimum radius for different values of n. The results for different values of n are

$$n = 2 \quad r_o = \frac{1}{2} \alpha_m \tag{56}$$
$$n = 3 \quad r_o = \left(-8\sqrt{3}\alpha_m \right) / \left(-24 + \sqrt{3}\alpha_m \right) \tag{57}$$
$$n = 4 \quad r_o = \frac{1}{4} \left(1 + \sqrt{2} \right) \alpha_m \tag{58}$$
$$n = 5 \quad r_o = \frac{1}{5} \left(\sqrt{5 + 2\sqrt{5}} \right) \alpha_m \tag{59}$$
$$n = 6 \quad r_o = \frac{1}{6} \left(2 + \sqrt{3} \right) \alpha_m \tag{60}$$
$$n = 8 \quad r_o = \frac{1}{8} \left(1 + \sqrt{2} + \left(\sqrt{2 - \sqrt{2}} + \sqrt{2 + \sqrt{2}} \right) \right) \alpha_m \tag{61}$$
$$n = 10 \quad r_o = \frac{1}{10} \left(1 + \sqrt{5} + \left(\sqrt{\frac{10}{4} - \frac{\sqrt{5}}{2}} + \sqrt{\frac{10}{4} + \frac{\sqrt{5}}{2}} \right) \right) \alpha_m \tag{62}$$
$$n = 12 \quad r_o = \frac{1}{12} \left(2 + \sqrt{2} + \sqrt{3} + \left(\sqrt{2 - \sqrt{3}} + \sqrt{2 + \sqrt{3}} \right) \right) \alpha_m \tag{63}$$

There are several interesting trends seen in the equations for r_o using different values of n. The equations are functions only of α_m. Therefore, the optimum configuration for a given n depends only on the ideal separation angle according to the instantaneous weight function w_α. The shape of the parabola does not affect the results. Furthermore, with the exception of $n = 3$, the optimum radii solutions are linear functions of α_m.

The relation between r_o and n is not immediately obvious. However, upon close inspection we can determine a more general form of r_o for several values of n. For $n = 2, 4, 6$ we can express r_o as

$$r_o = \frac{1}{n}\left(\frac{n-2}{2} + \sqrt{\frac{n}{2}}\right)\alpha_m \tag{64}$$

A plot of the optimum radius over a range of n values is seen in Figure 8. The points are the analytic solutions according to Eqs. (56–63) for $\alpha_m = 0.000375$ rad. The curve is a plot of the empirical solution in Eq. (64). The points for $n = 2, 4, 6$ fall exactly on the curve. This result is expected because the empirical function is derived from the equations of r_o for $n = 2, 4, 6$. The values of r_o for $n = 3, 5$ are in good agreement with the empirical solution. However, for $n > 8$ the accuracy of the empirical function degrades. The empirical function predicts a downward trend in r_o for $n > 8$. However, the analytic solution appears to approach a limiting value.

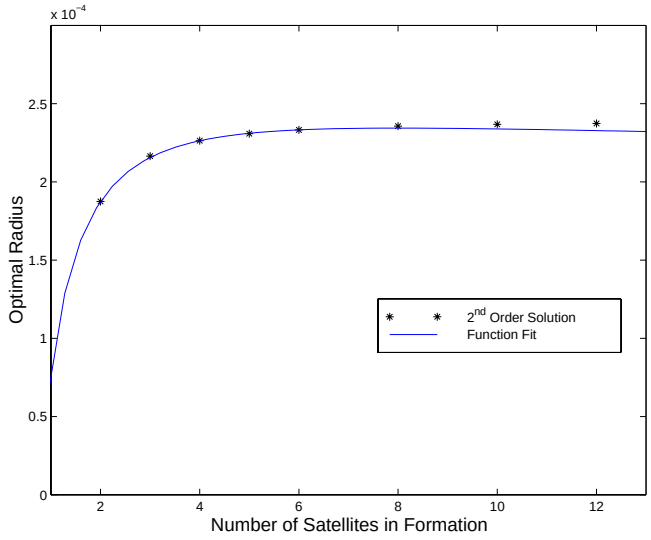

Figure 8: Optimum Radius for the Rotating Formation

We determine the limit of r_o as n approaches infinity using simple geometric relations. For $n \to \infty$, $w_p(\alpha_{ij})$ is the same for all i where $i \neq j$. Therefore we only need to evaluate $w_p(\alpha_{ij})$ for an arbitrary i. Thus for $n \to \infty$ we can write

$$\tilde{W}_\infty = \lim_{n\to\infty} \frac{1}{\eta_s} \sum_{i=1}^{n-1} \sum_{j=n+1}^{n} w_p(\alpha_{ij}) = \lim_{n\to\infty} \frac{1}{n-1} \sum_{j=2}^{n} w_p(\alpha_j) \tag{65}$$

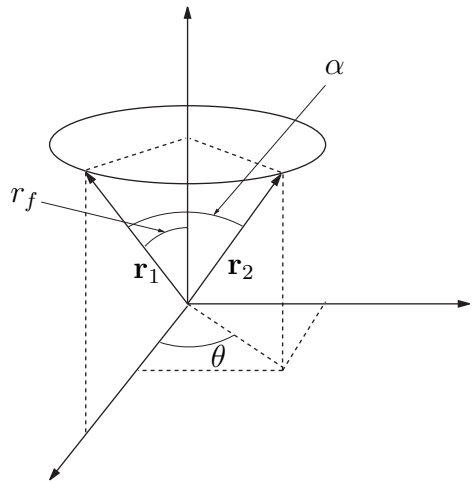

Figure 9: Circular Formation Geometry for $n = \infty$

Figure 9 shows two arbitrary radius vectors, $\mathbf{r}_1$ and $\mathbf{r}_2$, defining two spacecraft positions in a circular formation. Angle r_f is the angular radius of the formation. The angle around the circle between $\mathbf{r}_1$ and $\mathbf{r}_2$ is denoted θ. Using these definitions we can write Eq. (65) as

$$\tilde{W}_\infty = \lim_{n\to\infty} \frac{1}{n-1} \sum_{j=2}^{n} w_p(\alpha_j) = \frac{1}{2\pi} \int_0^{2\pi} w_p(\alpha) d\theta \tag{66}$$

From inspection of Figure 9 we can write

$$\mathbf{r}_1 = [\sin r_f \quad 0 \quad \cos r_f]^T \tag{67}$$

$$\mathbf{r}_2 = [\sin r_f \cos\theta \quad \sin r_f \sin\theta \quad \cos r_f]^T \tag{68}$$

Recall that W_α is not dependent on the semimajor axis. Therefore we use unit vector representations of the spacecraft positions without loss of generality. Using $r_1 = r_2 = 1$ we can express α as

$$\alpha = \| \mathbf{r}_1 \times \mathbf{r}_2 \| \tag{69}$$

for small α. Substituting Eqs. (67–68) into Eq. (69) we obtain

$$\alpha = \sqrt{\sin^2 r_f \left(-2\cos^2 r_f \left(-1 + \cos\theta\right) + \sin^2 r_f \sin^2\theta\right)} \tag{70}$$

Substituting Eqs. (70) and (54) into Eq. (49) we can evaluate the integral in Eq. (66):

$$\begin{aligned} \tilde{W}_\infty \;=\; & \frac{1}{16\pi\alpha_s} \left(-7\pi - 16\pi\alpha_l\alpha_u + 3\pi\cos 4r_f + 8\alpha_m(k_2 - k_1)\right) \\ & + \frac{1}{16\pi\alpha_s} \left(4\cos 2r_f \left(\pi + 2\alpha_m(k_2 - k_1)\right) + 32\alpha_m\sqrt{\sin^2 r_f}\right) \end{aligned} \tag{71}$$

where k_1 and k_2 are given by

$$k_1 = \ln\left[1 - \sqrt{\sin^2 r_f}\right] \tag{72}$$

$$k_2 = \ln\left[1 + \sqrt{\sin^2 r_f}\right] \tag{73}$$

To solve for the optimum radius as $n \to \infty$ we need to solve

$$\frac{\partial \tilde{W}_\infty}{\partial r_f} = 0 \tag{74}$$

However, the resulting derivative is a transcendental function in terms of α_m and r_f and cannot be explicitly solved for the optimum radius. Therefore we expand Eq. (71) in small r_f to second order:

$$\tilde{W}_\infty \approx \frac{1}{\alpha_s}\left(2r_f^2 - \frac{4\alpha_m r_f}{\pi} + \alpha_l \alpha_u\right) \tag{75}$$

We define r_∞ as the optimum radius as $n \to \infty$. Solving Eq. (75) for r_∞ we obtain

$$r_\infty = \frac{2}{\pi}\,\alpha_m \tag{76}$$

Like r_o for small n, r_∞ is only a function of α_m. Therefore the shape of the parabolic instantaneous weight function does not affect the optimum solution for large n. In Figure 10 the solution of r_o for a range of n values is plotted with the asymptote r_∞. The approximation for the asymptote is in good agreement with the analytic solution for r_o for large n.

Recall that several simplifying assumptions are made to obtain an analytic solution for W_α and the limiting value as $n \to \infty$. We need to determine if the simplifications yield solutions that are in good agreement with the exact solutions. Plots of W_α for $n = 3, 4, 8$, and 12 are shown in Figures 11–12 for a range of α_m. The data points are the exact numerical solutions for different radii obtained using a Runge-Kutta fourth order integrator to solve Eq.(21). The curves are the approximate analytic solutions for W_α. The approximate solutions are in excellent agreement with the exact solution for low α_m. For high α_m, on the order of $\alpha_m = 0.25$, accuracy of the approximate solution for W_α is poor. We expect a decrease in accuracy for high α_m because the small angle approximation was used in the development of the approximate solution. However, the optimum in performance occurs at nearly the same point according to both the exact and approximate solutions even for $\alpha_m = 0.25$. We see in Figure 13 plots of the exact *vs.* approximate optima for a range of α_m. The approximate solutions are accurate even for large α_m on the order of $\alpha_m = 0.5$. In the range of $0.5 < \alpha_m < 1$ the accuracy of the approximate solution degrades. However the approximate results are still useful in this range. We suggest that for $0.5 < \alpha_m < 1$ the approximate solutions be used as an initial guess to solve for the exact optimum using numerical techniques.

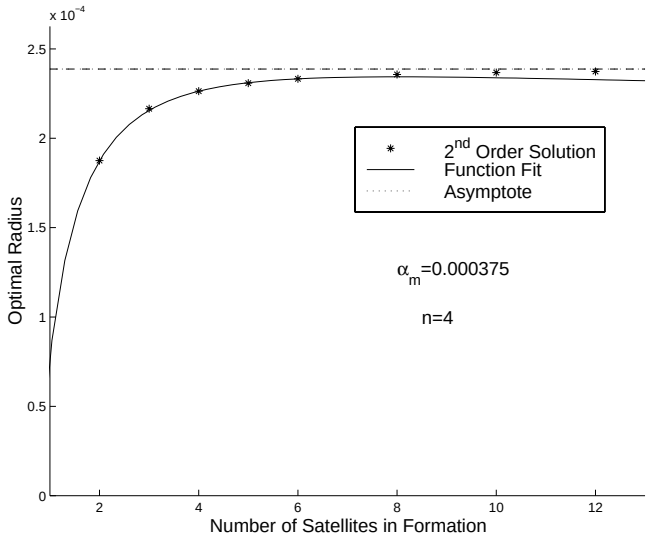

Figure 10: Optimum Radius with Asymptote *vs.* n

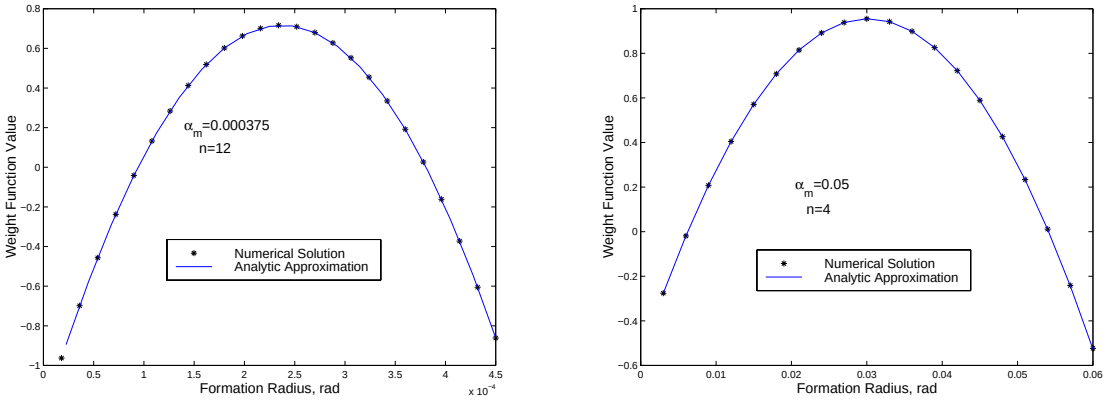

Figure 11: Approximate and Exact Solutions for W_α

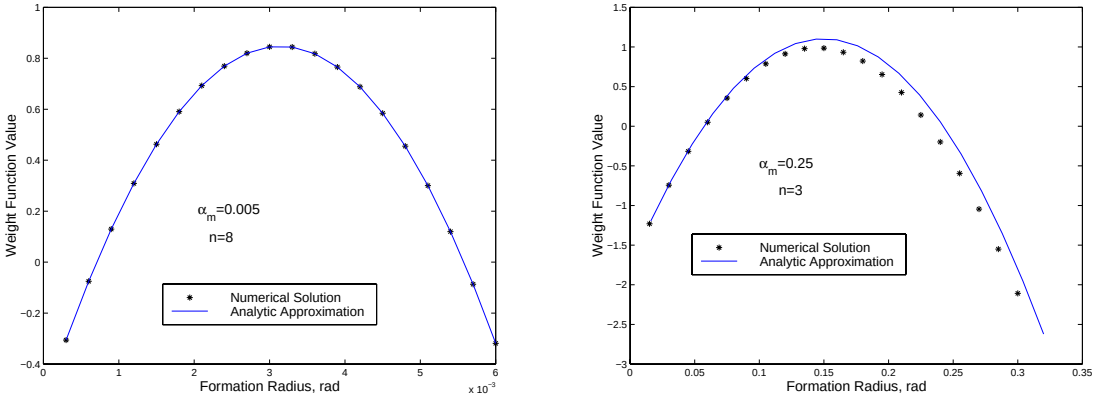

Figure 12: Approximate and Exact Solutions for W_α

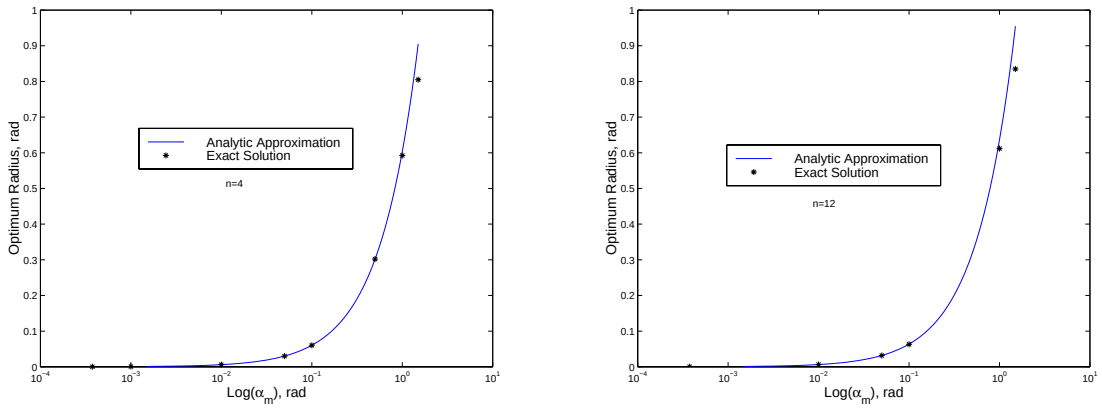

Figure 13: Approximate and Exact Optima *vs.* α_m

CONCLUSIONS

In this paper we develop an algorithm to place n satellites equally spaced in time around an ellipse in the relative reference frame in terms of the classical orbital elements. The dimensions of the ellipse-like path are shown to be simple functions of orbit eccentricity and inclination. We investigate the performance of the formation using a performance metric based on the orbit averaged sum of the angular separations between spacecraft. The exact expression is a non-trivial function of orbit eccentricity, inclination, the number of spacecraft, and the constants that define the instantaneous weight function. However, several simplifying assumptions allow for an analytic approximation. Using the resulting approximate equation for W_α we solve for optimal configurations for different values of n. We show that, according to the angular performance measure , the optimal rotating formation is circular. The optimal radii for different values of n are found to be simple functions of α_m, the ideal separation angle according to the instantaneous weight function. Interestingly, the optimal configuration does not depend on the shape of the parabola chosen for the instantaneous separation metric. For $n < 8$, the optimal radius is $r_o = ((n-2)/2 + \sqrt{n/2})\alpha_m/n$, whereas for large n (> 8), the asymptotic limit $r_o \to 2\alpha_m/\pi$ is quite accurate.

ACKNOWLEDGMENTS

The first author was supported by a grant from the Guidance Navigation and Control Center at NASA Goddard Space Flight Center, under the direction of David Folta and David Wiedow. The second author was supported by a grant from the Air Force Office of Scientific Research, under the direction of Arje Nachman.

NOTATION

a	semimajor axis, m
c_1, c_2, c_3	constants defining parabolic weight
d	spatial separation between two spacecraft, m
e	orbit eccentricity
$\mathcal{F}_I$	inertial reference frame
$\mathcal{F}_{rel}$	relative reference frame
$\mathcal{F}_R$	rotating reference frame
$\mathcal{F}_p$	perifocal reference frame
i	orbit inclination, rad
ℓ	true longitude at epoch, rad
n	number of spacecraft in formation
n_s	number of distinct angles in a formation
r_∞	optimum radius as $n \to \infty$, rad
r_o	optimum radius for rotating formation, rad
T	orbital period, s
t_i	propagation time for i^{th} spacecraft, s
t_s	equal time separation for n spacecraft, s
W_α	orbit performance measure
W_∞	W_α as $n \to \infty$
W_a	approximate expression for W_α
w_α	instantaneous position metric
α_{ij}	angle between the i^{th} and j^{th} satellites, rad
α_l	lower limit on angular separation, rad
α_m	ideal angular separation, rad
α_s	scaling factor, rad
α_u	upper limit on angular separation, rad
δ_{lon}	formation longitudinal separation, rad
δ_{lat}	formation latitudinal separation,rad
η	orbit mean motion, rad/s
ν	true anomaly, rad
Ω	longitude of ascending node, rad
ω	argument of periapsis, rad

REFERENCES

[1] Folta, D. C., Bordi, F., and Scolese, C., "Field of View Location for Formation Flying Polar Orbiting Missions," *Advances in Astronautical Sciences*, Vol. 75, No. 2, 1991, pp. 949–965.

[2] Folta, D. C., Bordi, F., and Scolese, C., "Considerations on Formation Flying Separations for Earth Observing Satellite Missions," *Advances in Astronautical Sciences*, Vol. 79, No. 2, 1992, pp. 803–822.

[3] Folta, D. C., Newman, L. K., and Gardner, T., "Foundations of Formation Flying for Mission to Planet Earth and New Millennium," In *Astrodynamics Conference Proceedings*, pp. 656–666, 1996.

[4] Decou, A. B., "Orbital Station-Keeping for Multiple Spacecraft Interferometry," *Journal of the Astronautical Sciences*, Vol. 39, No. 3, 1991, pp. 283–297.

[5] Gramling, C. J., Lee, T., Niklewski, D. J., and Long, A. C., "Relative Navigation for Autonomous Formation Flying Spacecraft," *Advances in Astronautical Sciences*, Vol. 97, No. 1, 1998, pp. 405–431.

[6] Hartman, K. R., Gramling, C. J., Lee, T., Kelbel, D. A., and Long, A. C., "Relative Navigation for Spacecraft Formation Flying," *Advances in Astronautical Sciences*, Vol. 100, No. 2, 1998, pp. 685–699.

[7] Guinn, J. R. and Boain, R. J., "Spacecraft Autonomous Navigation for Formation Flying Earth Orbiters Using GPS," In *Astrodynamics Conference Proceedings*, pp. 722–732, 1996.

[8] Adams, J., Robertson, A., Zimmerman, K., and How, J., "Technologies for Spacecraft Formation Flying," In *Proceedings of the Institute of Navigation GPS*, pp. 1321–1330, 1996.

[9] How, J. P., Twiggs, R., Weidow, D., Hartman, K., and Bauer, F., "Orion: A Low-Cost Demonstration of Formation Flying in Space Using GPS," In *Astrodynamics Conference Proceedings*, pp. 276–286, 1998.

[10] Vallado, D. A., *Fundamentals of Astrodynamics and Applications*, McGraw-Hill, New York, 1997.

[11] Chichka, D. F., "Dynamics of Clustered Satellites via Orbital Elements," In *AAS/AIAA Astrodynamics Specialist Conference Proceedings*, pp. 969–988, 1999.

[12] Hughes, S. P. and Hall, C. D., "Formation Flying Performance Measures for Earth Pointing Missions," In *Flight Mechanics Symposium*, pp. 309–318, 1999.